Bayesian Uncertainty Matching for Unsupervised Domain Adaptation

Jun Wen [1,2] , **Nenggan Zheng**[1,2*] , **Junsong Yuan**[3] , **Zhefeng Gong**[4] and **Changyou Chen**[3]

[1]Qiushi Academy for Advanced Studies, Zhejiang University, Hangzhou, China
[2]College of Computer Science and Technology, Zhejiang University, Hangzhou, China
[3]Computer Science and Engineering Department, State University of New York at Buffalo
[4]Department of Neurobiology, Zhejiang University School of Medicine, Hangzhou, China
{junwen,zfgong}@zju.edu.cn, zng@cs.zju.edu.cn, {jsyuan,changyou}@buffalo.edu

Abstract

Domain adaptation is an important technique to alleviate performance degradation caused by domain shift, e.g., when training and test data come from different domains. Most existing deep adaptation methods focus on reducing domain shift by matching marginal feature distributions through deep transformations on the input features, due to the unavailability of target domain labels. We show that domain shift may still exist via label distribution shift at the classifier, thus deteriorating model performances. To alleviate this issue, we propose an approximate joint distribution matching scheme by exploiting prediction uncertainty. Specifically, we use a Bayesian neural network to quantify prediction uncertainty of a classifier. By imposing distribution matching on both features and labels (via uncertainty), label distribution mismatching in source and target data is effectively alleviated, encouraging the classifier to produce consistent predictions across domains. We also propose a few techniques to improve our method by adaptively reweighting domain adaptation loss to achieve nontrivial distribution matching and stable training. Comparisons with state of the art unsupervised domain adaptation methods on three popular benchmark datasets demonstrate the superiority of our approach, especially on the effectiveness of alleviating negative transfer.

1 Introduction

Many machine-learning algorithms assume that training and test data, typically in terms of feature-label pairs, denoted as $\{x_i, y_i\}_i$, are drawn from the same feature-label space with the same distribution, where x_i is the feature while y_i is the label of x_i. However, this assumption rarely holds in practice as the data distribution is likely to change over time and space. Though state-of-the-art deep convolutional features have shown invariant to low-level variations to some degree, they are still susceptible to domain-shift, as it is expensive to manually label sufficient training data that cover diverse
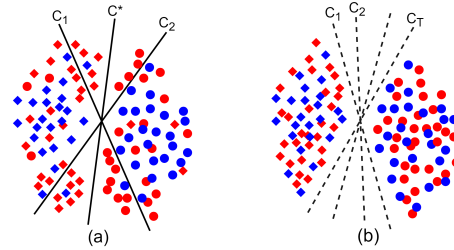

Figure 1: Comparisons between conventional and the proposed domain-adaptation methods (blue: source domain and red: target domain; diamonds and circles are samples from two different categories). Standard methods reduce domain-shift through *marginal feature-distribution* matching, which could learn a source-biased classifier C_1 or C_2 when the label-distributions do not match (C^* denotes a domain-invariant classifier). b) Our method jointly matches feature-distributions and label-distributions by learning domain-consistent probabilistic classifiers (sampled as $C_1, C_2, ..., C_T$) with uncertainty matching.

application domains. A typical solution is to further fine-tune a learned deep model on task-specific datasets. However, it is still prohibitively difficult and expensive to obtain enough labeled data for finetuning on a big deep network. Instead of re-collecting labeled data for every possible new task, unsupervised domain-adaptation methods are adopted to alleviate performance degradations by transferring knowledge from related labeled source domains to an unlabeled target domain [Ganin *et al.*, 2016; Li *et al.*, 2017; Zhou *et al.*, 2019].

When adopting domain adaptation, certain assumptions must be imposed on how distributions change across domains. For instance, most existing domain adaptation methods consider a covariate shift situation where the distributions on source and target domains only differ in the marginal feature-distribution $P(X)$, with an identical conditional distribution $P(Y|X)$ assumption. Here we use X and Y to denote random variables whose realizations are features x_i and labels y_i, either from the source data (X_s, Y_s) or target data (X_t, Y_t). In this setting, an early attempt is to match the feature distribution $P(X)$ on source and target domains by importance reweighting [Huang *et al.*, 2007]. State-of-the-art approaches reduce domain-shift by learning domain-invariant representations through deep neural transformations $\mathbf{G}_\phi(X)$, parameterized by ϕ, such that $P(\mathbf{G}_\phi(X_s)) \approx P(\mathbf{G}_\phi(X_t))$. This is often

*Corresponding author.

achieved by optimizing a deep network to minimize some distribution-discrepancy measures [Sun and Saenko, 2016; Tzeng *et al.*, 2017]. Because there is no target-domain label in the unsupervised domain adaptation scenario, most existing methods simply assume $P(Y_t|(\mathbf{G}_\phi(x_t))) \approx P(Y_s|(\mathbf{G}_\phi(x_s)))$ by sharing a classifier learned with source labeled data only. However, this is typically not true in practice as the source-learned classifier tends to be biased toward the source. As shown in Figure 1 (a), though the feature-distributions are well matched, the classifiers may still perform poorly in the target domain due to label-distribution mismatch.

In this paper, we alleviate the above problem by proposing an approximate joint-distribution matching scheme. Specifically, due to the lack of label information in a target domain, we propose to match the model prediction uncertainty, a second-order statistic equivalent, induced by the conditional distribution $P(Y|\mathbf{G}_\phi(X))$. We obtain the prediction uncertainty by imposing a Bayesian neural network (BNN) which induces posterior distributions over weights of a neural network. Without uncertainty matching, the BNN classifier is expected to produce high uncertainty for the unseen target-domain data and low uncertainty for the source-domain data, due to the bias induced by training on the source domain. By contrast, with prediction uncertainty matching, one is able to achieve an approximate joint-distribution matching, alleviating domain-shift on the classifier. The contributions of our work are summarized as follows:

- Different from most existing domain-adaptation methods, which only focus on reducing marginal feature-distribution discrepancy, we propose to match joint *feature-label distributions* by exploiting model prediction uncertainty, effectively alleviating conditional-distribution shift imposed by the classifier.

- We employ BNNs to quantify prediction uncertainty. Through additional source and target uncertainty discrepancy minimization, both fine-grained marginal feature-distribution and conditional label-distribution matching are achieved.

- Extensive experimental results on standard domain-adaptation benchmarks demonstrate the effectiveness of the proposed method, outperforming current state-of-the-art approaches.

2 Related Works

2.1 Domain Adaptation

Domain adaptation methods seek to learn discriminative features from neighbouring source domains to target domains. This is usually achieved by learning domain-invariant features [Ben-David *et al.*, 2010]. Previous methods usually seek to align source and target feature through subspace learning [Gong *et al.*, 2012]. Recently, deep adversarial-domain-adaptation approaches have taken over and achieved state-of-the-art performances [Hoffman *et al.*, 2018; Wen *et al.*, 2019]. These methods attempt to reduce domain discrepancy by optimizing deep networks with an adversarial objective produced by a discriminator network that is trained to distinguish features of target from source domains. Though

significant marginal distribution-shift can be reduced, these methods fail to fully address the conditional label-distribution shift problem. There are some recent models trying to address this issue by utilizing pseudo-labels [Long *et al.*, 2018; Chen *et al.*, 2018]. However, most of them are deterministic models, which can not essentially reduce the conditional domain-shift, due to the unavailability of target-domain labels.

2.2 Bayesian Uncertainty

Uncertainty can be achieved by adopting Bayesian neural networks. A typical BNN assigns a prior distribution, *e.g.*, a Gaussian prior distribution, over the weights, instead of deterministic weights as in standard neural networks. Given observed data, approximate inference is performed to calculate posterior distribution of the weights, such as the methods in [Graves, 2011; Blundell *et al.*, 2015]. A more effective way to calculate Bayesian uncertainty is to employ the dropout variational inference [Gal and Ghahramani, 2016], which is adopted in this paper.

3 The Proposed Method

3.1 The Overall Idea

Given a labeled source-domain dataset $D_s = (X_s, Y_s)$ and an unlabeled target-domain dataset $D_t = (X_t)$, the goal of unsupervised domain-adaptation is to learn an adapted model from the labeled source-domain data to the unlabeled target-domain data. The source and target domains are assumed to be sampled from two joint distributions $P_s(X_s, Y_s)$ and $P_t(X_t, Y_t)$, respectively, with $P_s \neq P_t$. The joint distribution of feature-label pairs can be decomposed as:

$$P(X, Y) = P(Y|X)P(X). \tag{1}$$

Limitations of Traditional Methods. Most existing domain-adaptation methods reduce domain-shift by learning a deep feature-transformation $\mathbf{G}_\phi$ such that $P(\mathbf{G}_\phi(X_s)) \approx P(\mathbf{G}_\phi(X_t))$, and a shared classifier network $P_\theta(Y_s|\mathbf{G}_\phi(X_s))$, parameterized by θ, using labeled source data D_s. To adapt to a target domain, the learned $P_\theta(Y_s|\mathbf{G}_\phi(X_s))$ is adopted to form the target-domain joint distribution $P(\mathbf{G}_\phi(X_t))P_\theta(Y_t|\mathbf{G}_\phi(X_t))$. It is easy to see that directly adopting $P_\theta(Y_s|\mathbf{G}_\phi(X_s))$ in the target-domain is unable to match the true joint distributions $P_s(X_s, Y_s)$ and $P_t(X_t, Y_t)$, as $P_\theta(Y_s|\mathbf{G}_\phi(X_s))$ only reflects feature-label information in the source domain.

Our Method

In this paper, we propose to jointly reduce the marginal-distribution shift $(P(X_s) \neq P(X_t))$ and conditional-distribution shift $(P(Y_s|X_s) \neq P(Y_t|X_t))$ by exploiting prediction uncertainty. Specifically, our model consists of a probabilistic BNN feature extractor $\mathbf{G}_\phi$ with inputs X_s or X_t, and a BNN classifier $\mathbf{C}_\theta$ with inputs $\mathbf{G}_\phi(X_s)$ or $\mathbf{G}_\phi(X_t)$. The classifier $\mathbf{C}_\theta$, which corresponds to the conditional distribution $P(Y|\mathbf{G}_\phi(X))$ and is parameterized by θ, learns to classify samples from both domains.

As discussed in the Introduction, directly learning to match $P(Y_s|\mathbf{G}_\phi(X_s))$ and $P(Y_t|\mathbf{G}_\phi(X_t))$ is unfeasible due to the unavailability of target labels. To overcome the difficulty, we
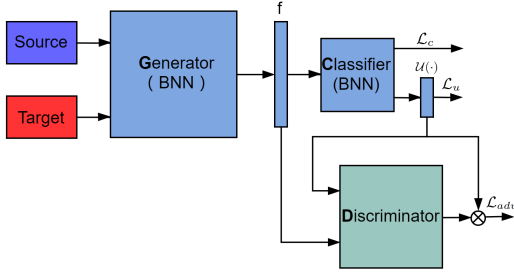
Figure 2: Pipeline of the proposed method. We adaptively match the joint distribution of the learned feature and prediction uncertainty.

instead learn to match the prediction uncertainty, a second-order statistics equivalent. The intuition is that if the second-order statistics of two distributions are matched, the two distributions will be brought closer. Another intuition is that, if target samples are not well matched with source samples in the feature space, these outliers are likely to be predicted with high uncertainty by a source-trained classifier. If one can quantify the uncertainty and minimize the cross-domain uncertainty discrepancy (source uncertainty is supposed to be low), the generator $\mathbf{G}_\phi$ will be encouraged to produce target features that best match the source both in the feature space and classifier prediction. In the following, we first introduce an effective way to obtain Bayesian uncertainty by adopting the dropout technique, and then describe the proposed framework of joint-distribution matching.

3.2 Bayesian Uncertainty

We employ Bayesian neural network (BNN) to quantify model prediction uncertainty. BNN is a variant of standard neural networks by treating the weights as distributions, instead of using deterministic weights. However, it is often computationally inhibited to perform inference on the weight distributions in a large-scale deep BNN. In this paper, we employ the practical dropout variational inference for approximate inference [Gal and Ghahramani, 2016] and efficient uncertainty approximation. In the proposed method, inference is done by training the model with dropout [Srivastava et al., 2014]. In testing, dropout is also performed to generate approximate samples from the posterior distribution. This approach is equivalent to using a Bernoulli variational distribution $q_\vartheta(\mathbf{W})$ [Gal and Ghahramani, 2016], parameterized by ϑ, to approximate the true model weights ($\mathbf{W}$) posterior. As proven in [Gal and Ghahramani, 2016], the dropout inference essentially minimizes the KL divergence between the approximate distribution and the posterior of a deep Gaussian process. For classification, the objective can be formulated as:

$$\mathcal{L}_{(\theta,p)} = -\frac{1}{N} \sum_{i=1}^{N} \log p(y_i | f^{\hat{\mathbf{W}}_i}(x_i)) + \frac{1-p}{2N} ||\vartheta||^2, \quad (2)$$

where N is the number of training samples, p denotes the dropout probability, $\hat{\mathbf{W}}_i$ is sampled according to the dropout variational distribution $q_\vartheta^*(\mathbf{W})$ [Gal and Ghahramani, 2016], and ϑ is the set of the variational distribution's parameters.

The final prediction can be obtained by marginalizing over the approximate posterior distribution on weights, which is

approximated using Monte Carlo integration as follows:

$$p(y_i = c|x_i, X, Y) = \frac{1}{T} \sum_{t=1}^{T} \mathsf{Softmax}(f^{\hat{\mathbf{W}}_t}(x_i)), \quad (3)$$

with T sampled masked weights, namely forwarding each sample x_i through the feature extractor $\mathbf{G}_\phi$ and classifier $\mathbf{C}_\theta$ for T times with weights sampled according to the dropout inference. The uncertainty of the prediction can be summarized using different metrics. In this paper, we use two metrics: 1) entropy of the averaged probabilistic prediction, and 2) variance of all prediction vectors. The entropy and variance based prediction uncertainty are denoted as $\mathcal{U}_{entro}$ and $\mathcal{U}_{var}$, respectively, formulated as:

$$\mathcal{U}_{entro}(x_i) = H(\frac{1}{T} \sum_{t=1}^{T} \mathsf{Softmax}(\mathbf{C}_\theta(\mathbf{G}_\phi(x_i))/\tau)), \quad (4)$$

$$\mathcal{U}_{var}(x_i) = \frac{1}{T} \sum_{t=1}^{T} (\mathbf{C}_\theta(\mathbf{G}_\phi(x_i)) - \frac{1}{T} \sum_{t=1}^{T} \mathbf{C}_\theta(\mathbf{G}_\phi(x_i)))^2, \quad (5)$$

where $H(\cdot)$ denotes the information entropy function and τ the temperature of the $Softmax$, which controls the uncertainty level.

3.3 Distribution Adaptation

In this section, we describe how to simultaneously alleviate the marginal and conditional domain-shift by matching the approximate joint distributions of the source and target feature-label pairs.

Joint-Distribution Adaptation

We employ adversarial learning to match source and target statistics to reduce distribution discrepancy, as adversarial domain-adaptation methods have achieved state-of-the-art performances [Goodfellow et al., 2014; Tzeng et al., 2017]. Basically, the procedure is described by a two-player game. The first player, a domain discriminator $\mathbf{D}$, is trained to distinguish source from target data; while the second player, the feature extractor $\mathbf{G}_\phi$, is trained to learn features that confuse the domain discriminator. By learning a best possible discriminator, the feature extractor is expected to learn features that are best domain-invariant. This learning procedure can be described by the following *minimax* game:

$$\min_{\mathbf{G}_\phi} \max_{\mathbf{D}} \mathcal{L}_{adv} = -\frac{1}{n_s} \sum_{i=1}^{n_s} (\log(\mathbf{D}(\mathbf{G}_\phi(x_i^s)))) \\ -\frac{1}{n_t} \sum_{i=1}^{n_t} (\log(1 - \mathbf{D}(\mathbf{G}_\phi(x_i^t)))), \quad (6)$$

where n_s and n_t are the number of training samples from source and target, respectively.

However, this typical adversarial *minimax* game for domain adaptation may be problematic in two aspects: 1) trivial feature alignment; and 2) unstable training. The domain discriminator fails to consider the relationship between learned features and the decision boundary of the classifier during feature alignment, which may lead to boundary target samples or trivial alignment with a huge-capacity $\mathbf{G}_\phi$ [Shu et al., 2018].

We aim to achieve nontrivial feature alignment by enforcing additional classifier prediction consistency during matching. Furthermore, noisy or hard-to-match samples may lead to unstable adversarial training. These confusing samples, which typically endow high prediction uncertainty, may produce unreliable gradients and deteriorate the training. They may also direct the $\mathbf{G}_\phi$ to learn features that is non-discriminative for classifying target samples, especially with a huge-capacity $\mathbf{G}_\phi$. Thus, we aim to attenuate the influence of noisy samples and reinforce the influence of easy-to-match target samples by adaptively re-weighting the adversarial loss. Specifically, we propose the following modified objective:

$$\min_{\mathbf{G}_\phi} \max_{\mathbf{D}} \mathcal{L}_{adv} = -\frac{1}{n_s} \sum_{i=1}^{n_s} (\alpha_{x_i^s} \log(\mathbf{D}(\mathbf{G}_\phi(x_i^s), \mathcal{U}(x_i^s)))) \\ -\frac{1}{n_t} \sum_{i=1}^{n_t} (\alpha_{x_i^t} \log(1 - \mathbf{D}(\mathbf{G}_\phi(x_i^t), \mathcal{U}(x_i^t)))), \quad (7)$$

where $\mathcal{U}(\cdot)$ is the prediction uncertainty formulated in Equation (4) or Equation (5). Both $\alpha_{x_i^s}$ and $\alpha_{x_i^t}$ are the adaptation loss weights, defined as:

$$\alpha_{x_i} = \begin{cases} 0 & \mathcal{U}(x_i) > t_u \\ \frac{N * e^{-\mathcal{U}(x_i)}}{\sum_{i=1}^{N} e^{-\mathcal{U}(x_i)}} & \mathcal{U}(x_i) \leq t_u, \end{cases} \quad (8)$$

where N is the number of training samples and t_u denotes the uncertainty threshold constraining the influence of samples with uncertainty larger than t_u. For samples with uncertainty less than t_u, the weights are normalized within each training batch with more attention paid on the certain samples. It is worth noting that we found directly using the uncertainty without normalization for the re-weighting as done in [Kendall and Gal, 2017; Long $et\ al.$, 2018] tend to discourage a model from predicting low uncertainty for all samples. With such an adaptive joint-distribution adaptation objective, we aim to achieve non-trivial feature alignment and enable safer transfer.

Conditional-Distribution Adaptation
Note the joint-distribution-matching scheme described in the last section does not necessarily guarantee a good conditional-distribution adaptation. In this section, we aim to reduce the conditional distribution shift and learn a domain-invariant classifier. Due to the infeasibility of directly minimizing the conditional distribution discrepancy $||P_\theta(Y|\mathbf{G}_\phi(X_s)) - P_\theta(Y|\mathbf{G}_\phi(X_t))||_q$, we propose to approximate it by matching prediction uncertainty, a second-order statistic equivalent, with a BNN as the classifier. We exploit prediction uncertainty to detect and quantify domain-shift of a classifier. By minimizing the uncertainty discrepancy between source and target, we aim to approximately reduce the domain-shift of the classifier, and the objective $\mathcal{L}_u$ can be formulated as :

$$\mathcal{L}_u = ||\mathcal{U}(X_s) - \mathcal{U}(X_t)||_q, \quad (9)$$

where we set $q = 2$ as we found it achieves better performances than $q = 1$. The prediction uncertainty discrepancy is estimated within each batch during training.

To enable discriminative feature transferring, the feature extractor $\mathbf{G}_\phi$ and classifier $\mathbf{C}_\theta$ are also trained to minimize the source supervised loss $\mathcal{L}_c$ using source labels, defined as:

$$\mathcal{L}_c = -\frac{1}{n_s} \sum_{i=1}^{n_s} y_i^s \cdot \log \mathsf{Softmax}(\mathbf{C}_\theta(\mathbf{G}_\phi(x_i^s))/\tau_c), \quad (10)$$

where y_i^s is the true label of the source sample x_i^s and τ_c is the $Softmax$ temperature for source classification.

Integrating all objectives together, the final learning procedure is formulated as:

$$\min_{\mathbf{G}_\phi, \mathbf{C}_\theta} \max_{\mathbf{D}} \mathcal{L}_{final} = \mathcal{L}_c + \lambda_{adv} \mathcal{L}_{adv} + \lambda_u \mathcal{L}_u, \quad (11)$$

where λ_{adv} and λ_u are hyper-parameters that trade-off the objectives in the unified optimization problem.

According to the analysis of [Ben-David $et\ al.$, 2010], the expected target error is upper-bounded by the following three terms: 1) source error, 2) domain divergence, and 3) conditional-distribution discrepancy across domains. We aim to improve marginal distribution matching to reduce the second term by minimizing $\mathcal{L}_{adv}$ to achieve joint feature-uncertainty adaptation. While the third term is ignored by most of existing domain adaptation methods, we are able to reduce it via uncertainty matching and $\mathcal{L}_u$ minimization.

4 Experiments

We compare our method with state-of-the-art domain-adaptation approaches on several benchmark datasets: *USPS-MNIST-SVHN* dataset [Hoffman $et\ al.$, 2018], *Office-31* dataset [Saenko $et\ al.$, 2010], and the recently introduced *Office-home* dataset [Venkateswara $et\ al.$, 2017].

USPS-MNIST-SVHN. This dataset is used for digits recognition with 3 domains: MNIST, USPS, and SVNH. MNIST is composed of grey images of size 28×28; USPS contains 16×16 grey digits; and SVHN consists of 32×32 color digits images, which are more challenging and might contain more than one digit in each image. We evaluate our method using the three typical adaptation tasks: USPS↔MNIST (two tasks) and SVHN→MNIST (one task). Following the same evaluation protocol of [Hoffman $et\ al.$, 2018], we use the standard training sets for domain-adaptation training and report adaptation results on the test sets.

Office-31. This dataset is widely used for visual domain adaptation [Saenko $et\ al.$, 2010]. It consists of 4,652 images and 31 categories collected from three different domains: Amazon (A) from amazon.com, Webcam (W) and DSLR (D), taken by web camera and digital SLR camera in different environmental settings, respectively. We evaluate all methods on the following four challenging settings: A↔W and A↔D.

Office-home. This is one of the most challenging visual domain adaptation datasets [Venkateswara $et\ al.$, 2017], which consists of 15,588 images with 65 categories of everyday objects in office and home settings. There are four significantly different domains: Art (Ar) consisting of 2427 painting, sketches or artistic depiction images, Clipart (Cl) containing 4365 images, Product (Pr) with 4439 images and Real-World (Rw) comprising of 4357 regularly captured images. We report performances of all the 12 adaptation tasks to enable thorough evaluations: Ar↔Cl, Ar↔Pr, Ar↔Rw, Cl↔Pr, Cl↔Rw, and Pr↔Rw.

Method	SVHN→MNIST	MNIST→USPS	USPS→MNIST	Avg
ADDA	76.0 ± 1.8	89.4 ± 0.2	90.1 ± 0.8	85.2
RAAN	89.2	89.0	92.1	90.1
LFPDA	86.9 ± 0.5	92.2 ± 0.4	92.5 ± 0.3	90.5
CyCADA	90.4 ± 0.4	95.6 ± 0.2	96.5 ± 0.1	94.2
CDAN-M	89.2	**96.5**	97.1	94.3
Ours(Var)	80.3 ± 0.7	93.5 ± 0.4	94.7 ± 0.3	89.5
Ours(Entro)	**91.5** ± 0.3	95.7 ± 0.4	**98.1** ± 0.2	**95.1**

Table 1: Accuracy (%) of unsupervised domain adaptation on digits recognition tasks.

Method	A→W	A→D	W→A	D→A	Avg
AlexNet	61.6 ± 0.4	63.8 ± 0.5	49.8 ± 0.4	51.1 ± 0.6	56.6
DANN	73.0 ± 0.5	72.3 ± 0.3	51.2 ± 0.5	53.4 ± 0.4	62.5
ADDA	73.5 ± 0.6	71.6 ± 0.4	53.5 ± 0.6	54.6 ± 0.5	63.3
LFPDA	75.2 ± 0.3	72.1 ± 0.5	54.2 ± 0.5	56.9 ± 0.5	64.6
JAN	74.9 ± 0.3	71.8 ± 0.2	55.0 ± 0.4	**58.3** ± 0.3	65.0
CDAN-M	78.3 ± 0.2	76.3 ± 0.1	**57.3** ± 0.3	57.3 ± 0.2	67.3
Ours(Entro)	**78.9** ± 0.4	**77.8** ± 0.3	56.6 ± 0.5	57.4 ± 0.4	**67.7**

Table 2: Accuracy (%) on the *Office31* dataset for unsupervised domain adaptation.

Compared Methods. The state-of-the-art deep domain-adaptation methods we compared include: Domain Adversarial Neural Network (DANN) [Ganin *et al.*, 2016], Adversarial Discriminative Domain Adaptation (ADDA) [Tzeng *et al.*, 2017], Joint Adaptation Networks(JAN) [Long *et al.*, 2017], Conditional Domain Adversarial Network (CADN) [Long *et al.*, 2018], Cycle-Consistent Adversarial Domain Adaptation (CyCADA) [Hoffman *et al.*, 2018], Re-weighted Adversarial Adaptation Network (RAAN) [Chen *et al.*, 2018], Local Feature Patterns for Domain Adaptation (LFPDA) [Wen *et al.*, 2019]. We follow standard evaluation protocols of unsupervised domain adaptation as in [Long *et al.*, 2017]. For our model, we report performances with uncertainty estimated with entropy and variance formulations, denoted as *Our(Entro)* and *Our(Var)*, respectively.

4.1 Implementation Details

CNN Architectures. For digit classification datasets, we use the same architecture as in ADDA [Tzeng *et al.*, 2017]. All digit images are resized to 28×28 for fair comparisons.

On the *Office-31* and the *Office-home* datasets, we finetune the AlexNet pre-trained from the ImageNet. Following the DANN [Ganin *et al.*, 2016], a bottleneck layer *fcb* with 256 units is added after the *fc7* layer for adaptation. We adopt the same image random flipping and cropping strategy as in JAN [Long *et al.*, 2017].

Hyper-parameters. To enable stable training, we progressively increase the importance of the adaptation loss and set $\lambda_{adv} = \frac{2}{1+\exp(\gamma \cdot m)} - 1$, where $\gamma = -10$ and m denotes the training progress ranging from 0 to 1. We use a similar hyper-parameter selection strategy as in DANN, called reverse validation. We set $\lambda_u = 0.25\lambda_{adv}$ to ensure uncertainty reduction. With $\tau = 1.5$, we forward each sample $T = 12$ times to obtain prediction uncertainty. We set $t_u = 0.2$, for adaptation loss re-weighting, and $\tau_c = 1.8$ for source classification loss. We dropout all fully-connected layers with a dropout ration

$q = 0.5$. Improvements are not observed with further dropout on convolution layers.

4.2 Results

The results on the digit recognition task are shown in Table 1. *Our(Entro)* achieves the best performances on most of the tasks. The CyCADA align features at both pixel-level and feature-level. RAAN alleviates conditional distribution shift by matching label distributions. CADN-M attempts to learn domain-invariant interactions between learned features and classifier through conditional adversarial learning. On these tasks, the plenty of source labels prevents the low-capacity *LeNet*-like model from overfitting the source labels, thus the advantages of our method over DAAN and CADN-M mainly come from uncertainty discrepancy minimization that alleviates the classifier bias.

Our(Entro) consistently outperforms *Our(Var)*. The distinct performance gap can be explained as follows. The entropy captures the cross-category probability spread of the prediction while the variance measures the deviation of prediction probabilities around the mean. The entropy uncertainty is more sensitive to the multi-peak probability spread across different categories. During training, the output probabilities of unmatched or boundary target samples usually cluster around two or more peaks, namely uncertain among several neighboring categories. In this case, the variance measure would obfuscate this multi-peak information. In the following, we only report the performances of *Our(Entro)*.

Performances on the *Office-31* and *Office-home* datasets are reported in Table 2 and Table 3, respectively. Again, our model achieves the best performances on most of the tasks. Due to the smaller size of the labeled source dataset and the huge capacity of the AlexNet, the models easily overfit the source labels while being jointly trained to reduce the marginal distribution discrepancy. The overfitting harms the transferability of the aligned features, resulting in learning trivial features for the target domain. In this case, our model alleviates this problem by jointly enforcing feature alignment and classifier prediction consistency.

Negative Transfer. Negative transfer happens when features are falsely aligned and domain adaptation causes deteriorated performances. Existing marginal distribution matching methods easily induce negative transfer when the marginal distributions between source and target are inherently different, *e.g.*, the source domain is smaller or larger than the target. We conduct experiments on the *Office-31* dataset with the *31→25* task by removing 6 classes from the target, and the *25→25(+6)* task by treating 6 extra target classes as noise images. We compare our method with DANN and *MADA* [Pei *et al.*, 2018] which is showed effective on alleviating negative transfer. The results are reported in Table 4. It is seen that DANN suffers obvious negative transfer on the *31→25* task. The effectiveness of our method on alleviating negative transfer is significant. Adaptive joint feature-uncertainty distribution matching encourages the model to mix source and target samples that best match with each other, thus alleviating the harmful effects of noisy samples.

Method	Ar→Cl	Ar→Pr	Ar→Rw	Cl→Ar	Cl→Pr	Cl→Rw	Pr→Ar	Pr→Cl	Pr→Rw	Rw→Ar	Rw→Cl	Rw→Pr	Avg
AlexNet	26.3	32.6	41.3	22.1	41.7	42.1	20.5	20.3	51.1	31.0	27.9	54.9	34.3
DANN	36.4	45.2	54.7	35.2	51.8	55.1	31.6	39.7	59.3	45.7	46.4	65.9	47.3
JAN	35.5	46.1	57.7	36.4	53.3	54.5	33.4	40.3	60.1	45.9	47.4	67.9	48.2
CDAN-M	38.1	50.3	60.3	**39.7**	56.4	57.8	**35.5**	43.1	**63.2**	48.4	48.5	71.1	51.0
Ours(Entro)	**40.3**	**51.6**	**61.5**	37.9	**58.0**	**58.6**	33.6	**45.9**	61.8	**50.1**	**50.9**	**71.7**	**51.8**

Table 3: Accuracy (%) on the *Office-home* dataset for unsupervised domain adaptation.

(a) Non-adapted (b) DANN (c) Ours(Entro) (d) DANN (e) Ours(Entro)
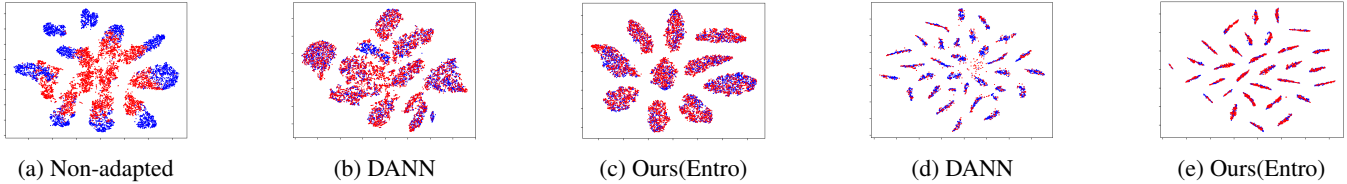
Figure 3: The t-SNE visualizations of features on the USPS→MNIST and A→D tasks (blue: source; red: target). (a) is trained without adaptation; (b) and (d) is trained with the typical adversarial domain adaptation method DANN. (c) and (e) adapted using our method. Our method significantly reduces the marginal discrepancy while with much less boundary target features comparing to DANN (best viewed in color).

Method	A→W	A→D	W→A	D→A	Avg
AlexNet	58.2(60.4)	60.4(61.5)	47.3(45.8)	49.8(49.3)	53.9(54.3)
DANN	65.1(70.7)	60.6(72.5)	42.9(46.9)	42.1(40.3)	52.7(57.6)
MADA	70.8(−)	69.6(−)	54.4(−)	54.2(−)	62.3(−)
Ours(Entro)	**73.4(76.2)**	**74.6(76.5)**	**55.5(54.8)**	**55.9(47.5)**	**64.9(63.8)**

Table 4: Accuracy (%) on the *Office31* dataset with *31→25* and *25→25(+6)* adaptation tasks. For the *25→25(+6)* task, the extra 6 classes are treated as noisy images. In the table, a in $a(b)$ denotes results of *31→25*, and b denotes results of *25→25(+6)*.
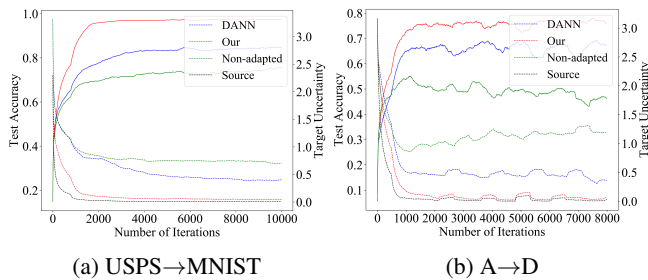

(a) USPS→MNIST (b) A→D

Figure 4: Comparisons of target test accuracy and uncertainty on the USPS→MNIST task and A→D task of the *Office31* dataset (dashed line: uncertainty; solid line: target test accuracy).

Alignment Visualization. We visualize the source and target learned representations on the USPS→MNIST and $A \rightarrow$D adaptation tasks using the t-SNE embedding [Maaten and Hinton, 2008]. In Figure 3, we visualize features of non-adapted models, DANN and our adapted model. Compared with the non-adapted model, DANN significantly reduces marginal distribution shift. Our method effectively prevents generating unmatched target samples that lie close to the decision boundary of the classifier and tend to be incorrectly classified.

Convergence and Uncertainty. In Figure 4, we show the convergence (test accuracy) and target uncertainty of the non-adapted model, DANN, and our model, on the USPS→MNIST and A→D tasks. As we can see, DANN adaptation effectively reduces target prediction uncertainty (source uncertainty is assured to be low) and improves target test accuracy. Our model further significantly reduces the discrepancy between source and target prediction uncertainty. The nearly synchronous increase of target accuracy and decrease of cross-domain prediction uncertainty discrepancy further indicates that uncertainty matching alleviates domain-shift and improves domain adaptation.

5 Conclusions

We have proposed a novel and effective approach for joint-distribution matching by exploiting prediction uncertainty. To achieve this, we adopt a Bayesian neural network to model prediction uncertainty. Unlike most of existing deep domain-adaptation methods that only reduce marginal feature-distribution shift, the proposed method additionally alleviates conditional distribution shift lingering in the last classifier. Experimental results verify the advantages of the proposed method over state-of-the-art unsupervised domain-adaptation approaches. More interestingly, we also have shown that the proposed method can effectively alleviate negative transfer in domain adaptation.

Acknowledgments

References

[Ben-David *et al.*, 2010] Shai Ben-David, John Blitzer, Koby Crammer, Alex Kulesza, Fernando Pereira, and Jennifer Wortman Vaughan. A theory of learning from different domains. *Machine learning*, 79(1-2):151–175, 2010.

[Blundell *et al.*, 2015] Charles Blundell, Julien Cornebise, Koray Kavukcuoglu, and Daan Wierstra. Weight uncertainty in neural network. In *International Conference on Machine Learning*, pages 1613–1622, 2015.

[Chen *et al.*, 2018] Qingchao Chen, Yang Liu, Zhaowen Wang, Ian Wassell, and Kevin Chetty. Re-weighted adversarial adaptation network for unsupervised domain adaptation. In *Proceedings of the IEEE Conference on Computer Vision and Pattern Recognition*, pages 7976–7985, 2018.

[Gal and Ghahramani, 2016] Yarin Gal and Zoubin Ghahramani. Dropout as a bayesian approximation: Representing model uncertainty in deep learning. In *international conference on machine learning*, pages 1050–1059, 2016.

[Ganin *et al.*, 2016] Yaroslav Ganin, Evgeniya Ustinova, Hana Ajakan, Pascal Germain, Hugo Larochelle, François Laviolette, Mario Marchand, and Victor Lempitsky. Domain-adversarial training of neural networks. *The Journal of Machine Learning Research*, 17(1):2096–2030, 2016.

[Gong *et al.*, 2012] Boqing Gong, Yuan Shi, Fei Sha, and Kristen Grauman. Geodesic flow kernel for unsupervised domain adaptation. In *Computer Vision and Pattern Recognition (CVPR), 2012 IEEE Conference on*, pages 2066–2073. IEEE, 2012.

[Goodfellow *et al.*, 2014] Ian Goodfellow, Jean Pouget-Abadie, Mehdi Mirza, Bing Xu, David Warde-Farley, Sherjil Ozair, Aaron Courville, and Yoshua Bengio. Generative adversarial nets. In *Advances in neural information processing systems*, pages 2672–2680, 2014.

[Graves, 2011] Alex Graves. Practical variational inference for neural networks. In *Advances in neural information processing systems*, pages 2348–2356, 2011.

[Hoffman *et al.*, 2018] Judy Hoffman, Eric Tzeng, Taesung Park, Jun-Yan Zhu, Phillip Isola, Kate Saenko, Alexei Efros, and Trevor Darrell. CyCADA: Cycle-consistent adversarial domain adaptation. In *Proceedings of the 35th International Conference on Machine Learning*, volume 80, pages 1989–1998. PMLR, 2018.

[Huang *et al.*, 2007] Jiayuan Huang, Arthur Gretton, Karsten M Borgwardt, Bernhard Schölkopf, and Alex J Smola. Correcting sample selection bias by unlabeled data. In *Advances in neural information processing systems*, pages 601–608, 2007.

[Kendall and Gal, 2017] Alex Kendall and Yarin Gal. What uncertainties do we need in bayesian deep learning for computer vision? In *Advances in neural information processing systems*, pages 5574–5584, 2017.

[Li *et al.*, 2017] Zheng Li, Yun Zhang, Ying Wei, Yuxiang Wu, and Qiang Yang. End-to-end adversarial memory network for cross-domain sentiment classification. In *IJCAI*, pages 2237–2243, 2017.

[Long *et al.*, 2017] Mingsheng Long, Han Zhu, Jianmin Wang, and Michael I Jordan. Deep transfer learning with joint adaptation networks. In *Proceedings of the 34th International Conference on Machine Learning-Volume 70*, pages 2208–2217. JMLR. org, 2017.

[Long *et al.*, 2018] Mingsheng Long, ZHANGJIE CAO, Jianmin Wang, and Michael I Jordan. Conditional adversarial domain adaptation. In *Advances in Neural Information Processing Systems 31*, pages 1647–1657. Curran Associates, Inc., 2018.

[Maaten and Hinton, 2008] Laurens van der Maaten and Geoffrey Hinton. Visualizing data using t-sne. *Journal of machine learning research*, 9(Nov):2579–2605, 2008.

[Pei *et al.*, 2018] Zhongyi Pei, Zhangjie Cao, Mingsheng Long, and Jianmin Wang. Multi-adversarial domain adaptation. In *AAAI Conference on Artificial Intelligence*, pages 3934–3941, 2018.

[Saenko *et al.*, 2010] Kate Saenko, Brian Kulis, Mario Fritz, and Trevor Darrell. Adapting visual category models to new domains. In *European conference on computer vision*, pages 213–226. Springer, 2010.

[Shu *et al.*, 2018] Rui Shu, Hung H Bui, Hirokazu Narui, and Stefano Ermon. A dirt-t approach to unsupervised domain adaptation. In *Proc. 6th International Conference on Learning Representations*, 2018.

[Srivastava *et al.*, 2014] Nitish Srivastava, Geoffrey Hinton, Alex Krizhevsky, Ilya Sutskever, and Ruslan Salakhutdinov. Dropout: a simple way to prevent neural networks from overfitting. *The Journal of Machine Learning Research*, 15(1):1929–1958, 2014.

[Sun and Saenko, 2016] Baochen Sun and Kate Saenko. Deep coral: Correlation alignment for deep domain adaptation. In *European Conference on Computer Vision*, pages 443–450. Springer, 2016.

[Tzeng *et al.*, 2017] Eric Tzeng, Judy Hoffman, Kate Saenko, and Trevor Darrell. Adversarial discriminative domain adaptation. In *Proceedings of the IEEE Conference on Computer Vision and Pattern Recognition*, pages 7167–7176, 2017.

[Venkateswara *et al.*, 2017] Hemanth Venkateswara, Jose Eusebio, Shayok Chakraborty, and Sethuraman Panchanathan. Deep hashing network for unsupervised domain adaptation. In *Proc. CVPR*, pages 5018–5027, 2017.

[Wen *et al.*, 2019] Jun Wen, Risheng Liu, Nenggan Zheng, Qian Zheng, Zhefeng Gong, and Junsong Yuan. Exploiting local feature patterns for unsupervised domain adaptation. In *Thirty-Third AAAI Conference on Artificial Intelligence*, 2019.

[Zhou *et al.*, 2019] Joey Tianyi Zhou, Ivor W. Tsang, Sinno Jialin Pan, and Mingkui Tan. Multi-class heterogeneous domain adaptation. *Journal of Machine Learning Research*, 20(57):1–31, 2019.